World Journal of Cardiology

Online Submissions: http://www.wjgnet.com/esps/
bpgoffice@wjgnet.com
doi:10.4330/wjc.v5.i12.444

World J Cardiol 2013 December 26; 5(12): 444-452
ISSN 1949-8462 (online)

TOPIC HIGHLIGHT

Zhonghua Sun, PhD, Associate Professor, *Series Editor*

Coronary CT angiography: Beyond morphological stenosis analysis

Zhonghua Sun

Zhonghua Sun, Discipline of Medical Imaging, Department of Imaging and Applied Physics, Curtin University, Perth, Western Australia 6845, Australia
Author contributions: Sun Z solely contributed to this paper.
Correspondence to: Zhonghua Sun, Associate Professor, Discipline of Medical Imaging, Department of Imaging and Applied Physics, Curtin University, GPO Box, U1987, Perth, Western Australia 6845, Australia. z.sun@curtin.edu.au
Telephone: +61-8-92667509 Fax: +61-8-92662377
Received: September 16, 2013 Revised: October 24, 2013
Accepted: November 18, 2013
Published online: December 26, 2013

Abstract

Rapid technological developments in computed tomography (CT) imaging technique have made coronary CT angiography an attractive imaging tool in the detection of coronary artery disease. Despite visualization of excellent anatomical details of the coronary lumen changes, coronary CT angiography does not provide hemodynamic changes caused by presence of plaques. Computational fluid dynamics (CFD) is a widely used method in the mechanical engineering field to solve complex problems through analysing fluid flow, heat transfer and associated phenomena by using computer simulations. In recent years, CFD is increasingly used in biomedical research due to high performance hardware and software. CFD techniques have been used to study cardiovascular hemodynamics through simulation tools to assist in predicting the behaviour of circulatory blood flow inside the human body. Blood flow plays a key role in the localization and progression of coronary artery disease. CFD simulation based on 3D luminal reconstructions can be used to analyse the local flow fields and flow profiling due to changes of vascular geometry, thus, identifying risk factors for development of coronary artery disease. The purpose of this article is to provide an overview of the coronary CT-derived CFD applications in coronary artery disease.

Key words: Computational fluid dynamics; Coronary artery disease; Hemodynamics; Modelling

Core tip: Coronary computed tomography (CT) angiography is limited to the visualization of anatomical details of coronary artery tree, while computational fluid dynamics (CFD) overcomes this limitation by providing hemodynamic changes to the coronary artery due to presence of plaques. CFD has been increasingly used in the investigation of cardiovascular disease due to its ability of providing flow changes and variations. This article provides an overview of the clinical applications of coronary CT-derived CFD in coronary artery disease.

Sun Z. Coronary CT angiography: Beyond morphological stenosis analysis. *World J Cardiol* 2013; 5(12): 444-452 Available from: URL: http://www.wjgnet.com/1949-8462/full/v5/i12/444.htm
DOI: http://dx.doi.org/10.4330/wjc.v5.i12.444

INTRODUCTION

Coronary artery disease (CAD) is the leading cause of death in advanced countries and its prevalence is increasing among developing countries[1]. Traditionally, diagnosis of CAD is performed by invasive coronary angiography which is considered the gold standard technique, since it has superior spatial and temporal resolution leading to excellent diagnostic accuracy. However, it is an invasive and expensive procedure associated with a small but distinct procedure-related morbidity (1.5%) and mortality (0.2%)[2]. Furthermore, invasive coronary angiography usually requires patients to stay for a short period in the hospital after the examination and this causes discomfort for the patients. Thus, a non-invasive technique for imaging and

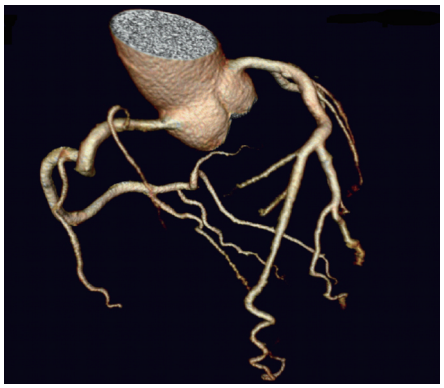

Figure 1 3D volume rendering shows normal right and left coronary arteries with excellent demonstration of main and side branches.

Figure 2 Curved planar reformation image shows significant stenosis of the left anterior descending coronary artery due to presence of plaques. The long arrow refers to the mixed plaque at the proximal segment of left left anterior descending (LAD), while the short arrow points to the calcified plaque at the proximal segment of LAD.

diagnosis of CAD is highly desirable.

Cardiac imaging has experienced rapid growth in recent years. Several techniques have been investigated for diagnosis and prognosis of patients with proven or suspected CAD. Although currently there is no less-invasive imaging modality that can replace invasive coronary angiography, the development of computed tomography (CT), magnetic resonance imaging (MRI), single photon emission computed tomography and positron emission tomography contribute to the detection and diagnosis of CAD less invasively when compared to the invasive coronary angiography[3-11].

Despite promising results achieved with these less-invasive modalities, the application is still limited to the visualization of anatomical details such as stenosis or occlusion, while the hemodynamic interference due to the presence of coronary plaques and subsequent flow changes cannot be assessed by traditional imaging techniques. Thus, identification of plaques that may cause cardiac events is of paramount importance for reducing the mortality and improving healthcare in patients suspected of CAD.

Computational fluid dynamics (CFD) enables analysis of hemodynamic changes of the blood vessel, even before the atherosclerotic plaques are actually formed in the artery wall. Therefore, to some extent, CFD allows for an early detection of atherosclerotic disease and improves understanding of the progression of plaques[12-14]. The purpose of this article is to provide an overview of the applications of CFD in the diagnosis of coronary artery disease based on coronary CT angiography examination.

CORONARY CT ANGIOGRAPHY VISUALIZATION OF CAD

Over the last decade a great deal of interest has been focused on imaging and diagnosis of CAD using coronary CT angiography due to its less invasive nature and improved spatial and temporal resolution (Figure 1). Moderate to high diagnostic accuracy was achieved with 64- or post-64 slice CT, owing to further technical improvements[15-19]. These studies have indicated that coronary CT angiography has high accuracy for the diagnosis of CAD and could be used as an effective alternative to invasive coronary angiography in selected patients (Figure 2).

In addition to the diagnostic value, coronary CT angiography demonstrates the potential to visualize coronary artery wall morphology, characterize atherosclerotic plaques and identify non-stenotic plaques that may be undetected by invasive coronary angiography (Figure 3). Studies have shown that coronary CT angiography demonstrates high prognostic value in CAD, as it is able to differentiate low-risk from high-risk patients, with very low rate of adverse cardiac events occurring in patients with normal coronary CT angiography, and significantly high rate of these events in patients with obstructive CAD[20-22].

According to the guidelines of the European Society of Cardiology, and the American College of Cardiology/American Heart Association, the decision to perform interventional procedures such as coronary angioplasty or bypass surgery should integrate anatomical information with a test that provides objective proof of ischemia[23,24]. Echocardiography is a multimodality imaging technique which allows accurate assessment of myocardial structure, function and perfusion. Stress echocardiography has become widely used for evaluation of patients with suspected or known CAD, and it has been reported to be a cost-effective and feasible modality in the diagnosis of CAD[25,26]. Although coronary CT angiography has been reported to provide potentially important additional information on myocardial perfusion and chronic myocardial infarction, a limited correlation between stenotic coronary disease and single photon emission computed tomography (SPECT) findings was noticed[27]. However, with the emergence of dual-energy CT (DECT), which offers fascinating new applications such as the mapping of the iodine distribution, acquisition of both anatomic and functional information is possible[28,29]. Early studies have reported that DECT had more than 90% diagnostic accuracy for detecting myocardial perfusion defect compared to myocardial perfusion SPECT imaging[29,30], although large patient cohorts are needed to confirm the potential application of DECT

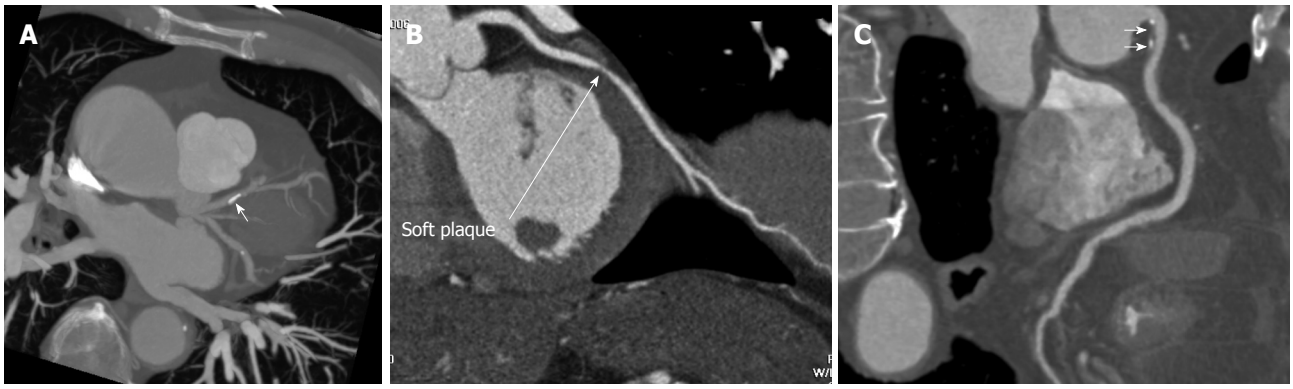

Figure 3 Characterization of coronary plaques on coronary computed tomography angiography. Coronal maximum intensity projection shows a calcified plaque (A, arrow) at the proximal segment of left coronary artery. A non-calcified plaque is present at the mid-segment of right coronary artery (B, arrow) on a curved planar reformation image. A mixed plaque is present at the proximal segment of right coronary artery (C, arrows) on a curved planar reformation image.

for both anatomic and myocardial perfusion assessment of CAD.

Coronary CT angiography provides excellent views of anatomical changes of the artery wall due to presence of plaques, thus enabling assessment of the degree of coronary stenosis. Coronary CT angiography claims to not only identify flow-limiting coronary stenosis, but also detect calcified and non-calcified plaques, measure atherosclerotic plaque burden and its response to treatment, and differentiate stable plaques from those that tend to rupture[31,32]. However, these expectations have not yet been met. In contrast, CFD enables analysis of hemodynamic changes of the blood vessel, thus improving our understanding of the progression of plaques formation and development of atherosclerosis.

COMPUTATIONAL FLUID DYNAMICS

CFD is a general term of all numerical techniques that are used to describe and analyse the flow of fluid elements at each location in certain geometry. The basic principle in CFD is that a complex geometry is separated into a large number of small finite elements. Those elements create a grid on which the equations describing the flow are analysed. The merit of CFD is developing new and improved devices and system designs, and optimization is conducted on existing equipment through computational simulations resulting in enhanced efficiency and lower operating costs[33]. However, CFD is still emerging in the biomedical field due to complexity of human anatomy and human body fluid behaviour. With high performance hardware and software easily available due to advances in computer science, biomedical research with CFD has become more accessible in recent years[34].

APPLICATIONS OF CFD IN CAD

Recently, CFD techniques have been increasingly used to study cardiovascular hemodynamics through simulation tools to assist in predicting the behaviour of circulatory blood flow inside the human body. Mechanical forces and intravascular hemodynamics can chronically affect and regulate blood vessels structure which induces a chronic inflammatory response in the arterial walls resulting in atherosclerosis[35,36]. Early CFD-based hemodynamic studies were conducted to represent *in vitro* conditions within restrictive assumptions[37-40]. Later reports demonstrated that CFD methods have the potential to enhance the data obtained from *in vivo* methods (CT or MRI) by providing a complete characterization of hemodynamic conditions (blood velocity and pressure as a function of space and time) under precisely controlled conditions (Figure 4)[41-44].

Knight *et al*[41] performed an analysis of the hemodynamic parameters including average wall-shear stress gradient, wall shear stress and oscillatory shear index obtained through a CFD study on the right coronary arteries of 30 patients. These parameters were correlated to each patient's specific plaque profile with aim of predicting the particular plaque location. Their results showed a statistically significant difference between average wall shear stress and oscillatory shear index in sensitivity and positive predictive value for the identification of atherosclerotic plaque sites in the right coronary artery. These findings further strengthen the theory that low shear stress is a contributor to the initiation of atherosclerosis.

In addition to the CFD analysis of main coronary arteries, impact of side branches on local wall shear stress should not be neglected. Wellnhofer *et al*[42] studied the impact of side branches on wall shear stress calculation in 17 patients and they concluded that side branches showed significant impact on coronary flow and wall shear stress profile in the right coronary artery. In contrast, Chaichana *et al*[43] investigated the influence of realistic coronary plaques on coronary side branches, based on a sample patient with coronary artery stenosis at the left coronary bifurcation. A direct correlation was found between coronary plaques and subsequent wall shear stress and wall pressure stress gradient changes in the coronary side branches (Figure 5). These research findings improve the understanding of the development of

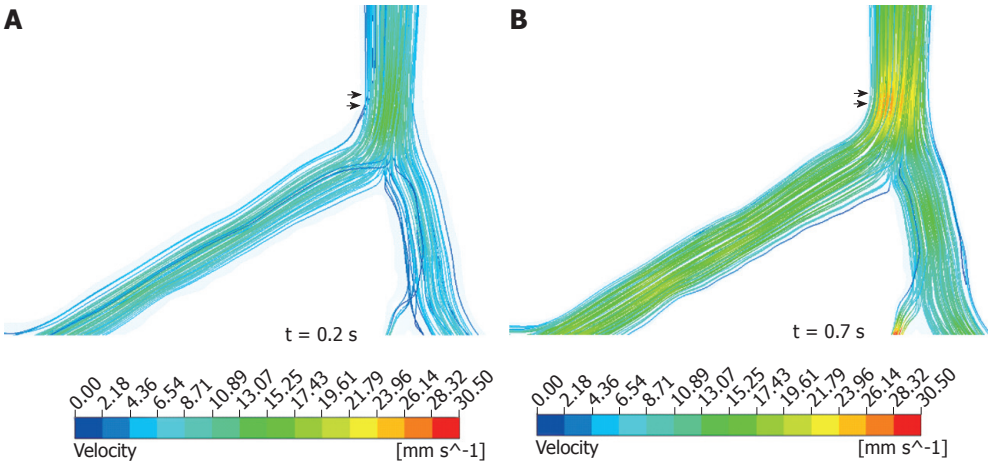

Figure 4 Local impact of flow velocity observed in a normal coronary model during systolic phase of 0.2 s (A) and diastolic phase of 0.7 s (B). Double arrows reveal high flow velocity locations at bifurcation in the left coronary artery model.

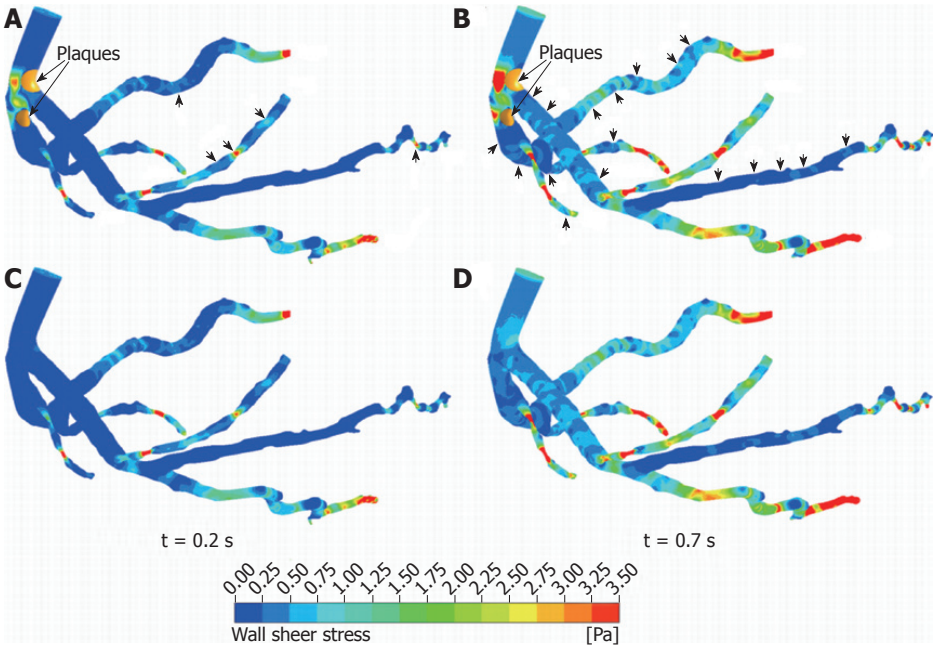

Figure 5 Computational fluid dynamics analysis of wall shear stress in 3D realistic models generated from coronary computed tomography angiography during systolic phase of 0.2 s and diastolic phase of 0.7 s. A, B: Coronary models with presence of plaques in the left anterior descending; C, D: Computational fluid dynamics analysis simulation in coronary models without presence of plaques. Arrows indicate the effect of plaques locations on wall shear stress changes in coronary side branches in the post-plaques-conditions.

atherosclerosis by exploring the hemodynamic effect of coronary plaques using CFD technique, although further studies based on a large cohort are required to verify these results.

Hemodynamic effect of left coronary angulation

The natural history of coronary plaque is dependent not only on the formation and progression of atherosclerosis, but also on the vascular remodelling response. If the local wall shear stress is low, a proliferative plaque will form. Local inflammatory response will stimulate the formation of so-called "vulnerable plaque" which is prone to rupture with superimposed thrombus formation. The vast majority of these inflamed high-risk vulnerable plaques cannot be detected by anatomic imaging and myocardial perfusion imaging. Since the progression and development of vulnerable plaque is associated with low wall shear stress and the presence of expansive remodelling, measurement of these characteristics *in vivo* will enable risk stratification for the entire coronary circulation[12,13,44]. Wong *et al*[45] simulated plaque locations in different angles involving ten patterns of plaques formation in the coronary artery wall, and they studied the effects of blood flow resistance through diseased coronary artery. Their proposed formation of the wall geometry has potential applications in the provision of reduction of flow estimates in angiography equipment and in situations where practical experimental measurement of the

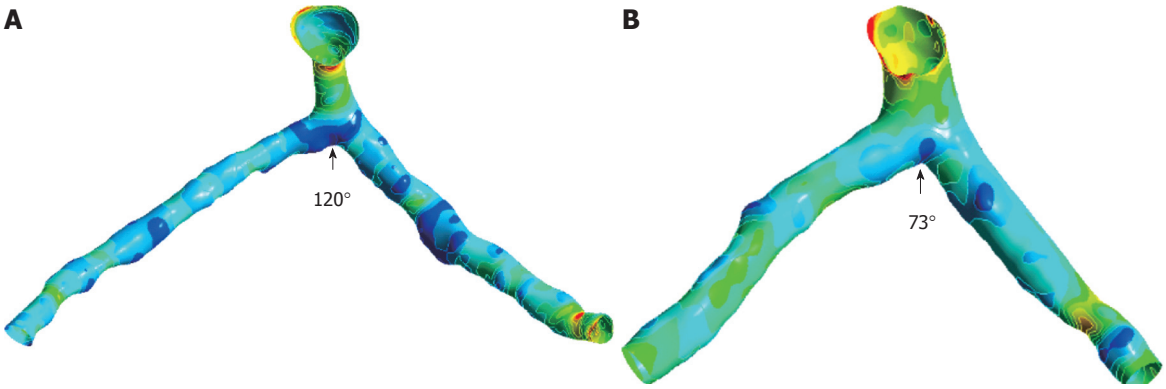

Figure 6 Wall shear stress gradient observed with different angles of the realistic left coronary artery models generated from coronary computed tomography angiography at peak systolic phase of 0.4 s. The arrows display the wall shear stress gradient distributions, with a large region of the low magnitude present at present at a 120° model (A) and a small region at a 73° model (B).

flow is unavailable.

The strong correlation between averaged low wall shear stress and the localization of atherosclerotic lesions in arterial bifurcations has been well established[12,46,47]. Rodriguez-Granillo *et al*[47] in their prospective study reported that atherosclerotic plaques located in the ostial left anterior descending coronary artery demonstrated larger plaque burden, maximal plaque thickness and low shear stress than those located in the distal left main coronary artery. Chaichana *et al*[48] in their recent study based on simulated and realistic coronary models showed a direct relationship between angulations of the left coronary artery and corresponding hemodynamic changes. Low wall shear stress and wall shear stress gradient was observed in the wide-angled models ranging from 75° to 120° when compared to the narrow-angled models ranging from 15° to 60°. Similarly, the magnitude of wall shear stress was significantly lower in the wide angulation models (120° and 110°) than that observed in the narrow angulation models (58°) which were generated based on patient's coronary CT images (Figure 6). This emphasises the potential risk of developing atherosclerosis at the left coronary bifurcation, although further studies are needed to validate these results in more realistic patient' data.

Hemodynamic effect of plaque location at the left coronary artery

Coronary plaque generally originates in the bifurcation region due to the angulations. The angulations cause a region of low wall shear stress, as confirmed by previous reports[48-53]. Medical imaging modalities such as intravascular ultrasound and coronary CT angiography have been commonly used to detect plaque locations in the left main coronary artery[54,55]. These imaging techniques provide valuable diagnostic information, such as assessment of plaque components and corresponding coronary lumen changes, however, they offer no tangible insight into the resultant hemodynamics. CFD provides an opportunity to predict the hemodynamic behaviour. Thus, the characterization of hemodynamic variations due to the various types of bifurcation plaque in the configurations can be further explored with flow visualizations; this exceeds the traditional anatomical analysis of coronary stenosis or occlusion.

According to a recent study by Chaichana *et al*[56], various types of plaques were simulated in different positions of the left coronary artery to reflect the realistic distribution of coronary plaques, as shown in Figure 7A. The wall shear stress, velocity and pressure gradient were computed and compared using CFD method. Figure 7B shows hemodynamic effects corresponding to different types of plaque in the left coronary artery, with significant difference among these plaques, while Figure 7C demonstrates the pressure gradient variations in relation to the plaque locations. These findings indicate that extra plaque located in the left coronary artery may increase the risk of plaque rupture, although further studies are needed to analyse the realistic plaque at the coronary artery based on different configurations (concentric *vs* eccentric plaques) and compositions (calcified *vs* non-calcified plaques).

Coronary CT angiography-derived fractional flow reserve

A technique to reveal the culprit CAD during invasive coronary angiography is the fractional flow reserve (FFR) measurement using a pressure-sensing guiding wire. FFR is the gold standard assessment of the hemodynamic significance of coronary stenoses as it is a measurement of the functional severity of a stenosis based on the pressure changes over a lesion during maximal coronary hyperemia. FFR is defined as maximal blood flow in a stenotic artery as a ratio to normal maximal flow[57]. FFR is measured at the time of invasive coronary angiography. An FFR of 0.80 is used as a cut off value to determine coronary stenoses responsible for ischemia with an accuracy of more than 90%[58,59]. FFR has been shown to improve detection of lesions that cause ischemia when compared with coronary CT angiography stenosis, thus, reducing the rates of false positive lesions incorrectly classified by stenosis alone[60].

Computation of FFR_{CT} is performed by computational fluid dynamics modelling after segmentation of coronary arteries and left ventricular myocardium. 3D

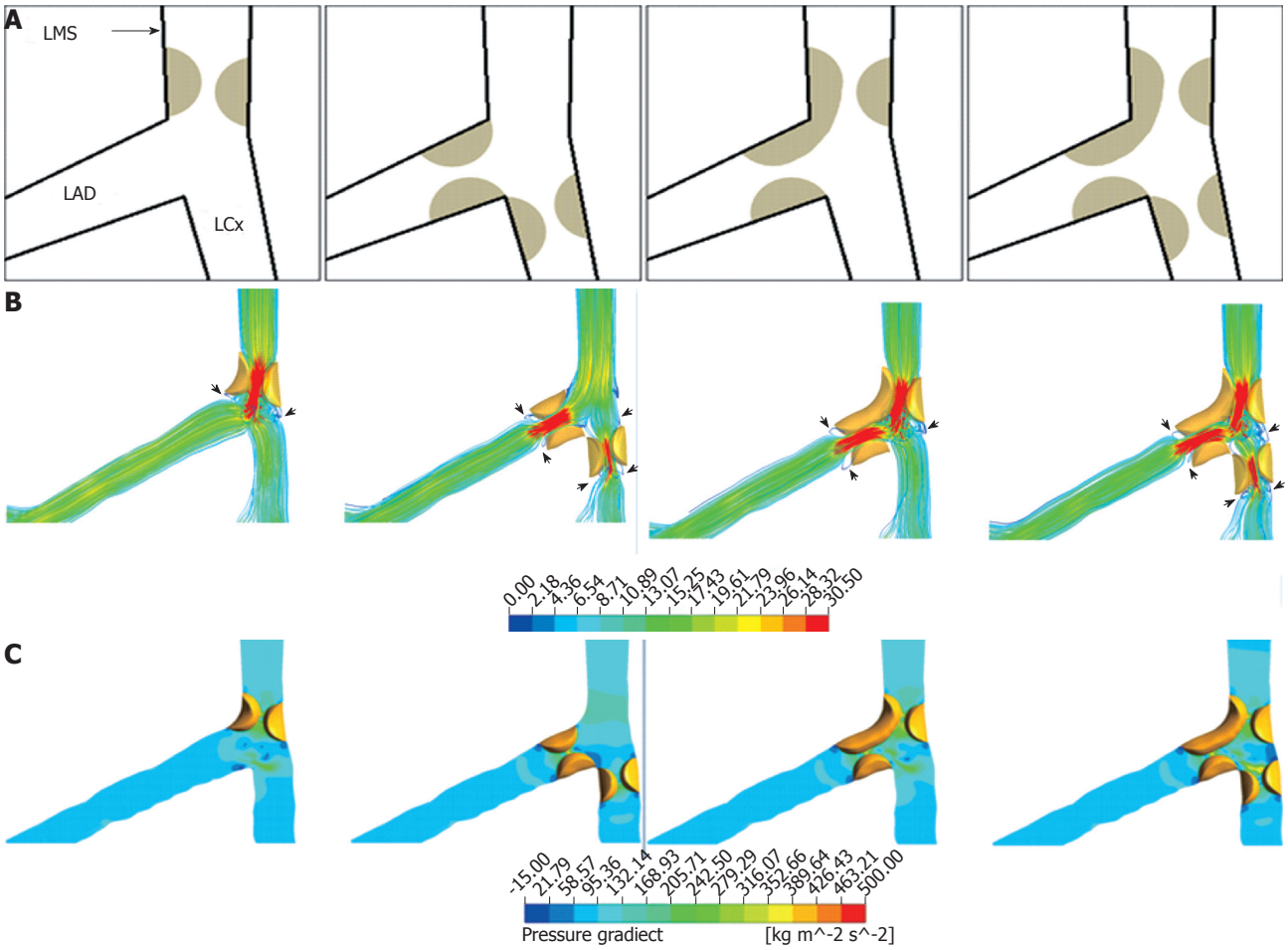

Figure 7 Computational fluid dynamics simulation of left coronary models with measurement of flow velocity and pressure gradient. A: Diagram shows characterization of the four different types of bifurcation plaques in the left coronary artery; B: The velocity patterns inside left bifurcation at effective plaque locations with these types of bifurcation plaques during the diastolic phase (0.7 s); C: The pressure gradient patterns inside left bifurcation at plaque locations with different types of bifurcation plaques during the systolic phase (0.2 s) (C). Arrows refer to the flow changes in the location of plaques. It is noticed that high velocity and high pressure gradient are present in the models with more plaques formed in the left coronary artery branches. LMS: Left main stem; LAD: Left anterior descending; LCx: Left circumflex.

blood flow simulations of the coronary arteries are performed with blood modelled as a Newtonian fluid using incompressible Navier-Stokes equations, with implementation of appropriate initial and boundary conditions to the models using a finite element method on a supercomputer. In order to ensure that the analysis reflects the realistic simulation *in vivo* conditions, realistic physiological boundary conditions are applied for 3D numerical analysis. The transient simulation is performed using accurate hemodynamic rheological and material properties, as described in previous studies[43,48]. Coronary blood flow is simulated under conditions modelling adenosine-mediated coronary hyperemia. The FFR$_{CT}$ ratio is obtained by dividing the mean pressure distal to the coronary stenosis by the mean aortic pressure, which can be measured during CFD simulations.

The FFR measurement was tested with coronary CT angiography and CFD technique and results are promising[61-63]. Min *et al*[61] in their multicenter study involving 252 stable patients with suspected or known CAD compared CT-derived FFR (FFR$_{CT}$) with coronary CT angiography and invasive coronary angiography for the diagnosis of hemodynamically significant coronary stenosis. Their results showed that FFR$_{CT}$ is considered a potentially promising non-invasive method for identification of individuals with ischemia. FFR$_{CT}$ plus CT improved diagnostic performance in terms of sensitivity and specificity when compared to CT alone. Similarly, Koo *et al*[62] in their DISCOVER-FLOW multicenter study further confirmed the usefulness of FFR derived from coronary CT angiography in the identification of ischemic coronary stenosis. On a per-vessel analysis (FFR$_{CT}$ was performed on 159 vessels in 103 patients), the diagnostic accuracy, sensitivity, specificity, positive predictive value and negative predictive value were 84.3%, 87.9%, 82.2%, 73.9%, 92.2%, respectively, for FFR$_{CT}$, and were 58.5%, 91.4%, 39.6%, 46.5%, 88.9%, respectively, for coronary CT angiography. These findings together with others indicate that FFR computed from coronary CT angiography provides better diagnostic performance for the diagnosis of lesion-specific ischemia and offers incremental value for the depiction of the culprit lesion in CAD compared to

coronary CT angiography[62-65]. In addition to the assessment of coronary stenosis, FFR_{CT} could be further applied to evaluate the in-stent restenosis or for coronary artery bypass grafts, although reports are limited in these areas.

Despite the promising results of FFR_{CT} in the detection of flow-limiting coronary stenosis, this technique suffers from some limitations. In order to confirm the diagnostic accuracy of FFR_{CT}, it needs to be compared with the gold standard, FFR which is measured by invasive coronary angiography. Furthermore, coronary CT angiography is associated with high radiation dose, although dose-reduction strategies have been recommended to reduce radiation exposure to patients[15]. Currently, myocardial perfusion SPECT imaging remains a widely accepted technique for functional assessment of coronary artery disease[27].

SUMMARY AND CONCLUSION

Although many risk factors predispose development of atherosclerosis, it tends to develop at locations where disturbed flow patterns occur, suggesting that lesion-prone areas may be due to biomechanically related factors. Furthermore, regional hemodynamics such as flow velocity, wall shear stress and wall pressure have been regarded as other risk factors for developing coronary artery disease[66-69].

CFD has been increasingly used to analyse coronary artery hemodynamics and implicate atherosclerosis progression. CFD method applied to coronary CT angiography has enabled non-invasive assessment of lesion-specific ischemia by FFR_{CT}. Furthermore, these methods also assist prediction of changes in coronary flow and pressure from therapeutic procedures (*e.g.*, percutaneous coronary intervention, coronary artery bypass graft)[70]. More research is being conducted on realistic *in vivo* coronary geometry models, and it is expected that research findings will provide potential valuable information for improving our understanding of the biomechanical pathophysiology of atherosclerosis and its complications.

REFERENCES

1 **American Heart Association**, American Stroke Association. 2002 Heart disease and stroke statistical update. Dallas, Texas: The American Heart Association, 2002

2 **Noto TJ**, Johnson LW, Krone R, Weaver WF, Clark DA, Kramer JR, Vetrovec GW. Cardiac catheterization 1990: a report of the Registry of the Society for Cardiac Angiography and Interventions (SCA& amp; I). *Cathet Cardiovasc Diagn* 1991; **24**: 75-83 [PMID: 1742788]

3 **Hingorani A**, Ascher E, Marks N. Preprocedural imaging: new options to reduce need for contrast angiography. *Semin Vasc Surg* 2007; **20**: 15-28 [PMID: 17386360 DOI: 10.1053/j.semvascsurg.2007.02.005]

4 **Sun Z**, Jiang W. Diagnostic value of multislice computed tomography angiography in coronary artery disease: a meta-analysis. *Eur J Radiol* 2006; **60**: 279-286 [PMID: 16887313 DOI: 10.1016/j.ejrad.2006.06.009]

5 **Sun Z**, Lin C, Davidson R, Dong C, Liao Y. Diagnostic value of 64-slice CT angiography in coronary artery disease: a systematic review. *Eur J Radiol* 2008; **67**: 78-84 [PMID: 17766073 DOI: 10.1016/j.ejrad.2007.07.014]

6 **Sommer T**, Hackenbroch M, Hofer U, Schmiedel A, Willinek WA, Flacke S, Gieseke J, Träber F, Fimmers R, Litt H, Schild H. Coronary MR angiography at 3.0 T versus that at 1.5 T: initial results in patients suspected of having coronary artery disease. *Radiology* 2005; **234**: 718-725 [PMID: 15665221 DOI: 10.1148/radiol.2343031784]

7 **Stuber M**, Botnar RM, Fischer SE, Lamerichs R, Smink J, Harvey P, Manning WJ. Preliminary report on in vivo coronary MRA at 3 Tesla in humans. *Magn Reson Med* 2002; **48**: 425-429 [PMID: 12210906 DOI: 10.1002/mrm.10240]

8 **Hachamovitch R**, Berman DS, Shaw LJ, Kiat H, Cohen I, Cabico JA, Friedman J, Diamond GA. Incremental prognostic value of myocardial perfusion single photon emission computed tomography for the prediction of cardiac death: differential stratification for risk of cardiac death and myocardial infarction. *Circulation* 1998; **97**: 535-543 [PMID: 9494023]

9 **van der Vaart MG**, Meerwaldt R, Slart RH, van Dam GM, Tio RA, Zeebregts CJ. Application of PET/SPECT imaging in vascular disease. *Eur J Vasc Endovasc Surg* 2008; **35**: 507-513 [PMID: 18180182 DOI: 10.1016/j.ejvs.2007.11.016]

10 **Husmann L**, Wiegand M, Valenta I, Gaemperli O, Schepis T, Siegrist PT, Namdar M, Wyss CA, Alkadhi H, Kaufmann PA. Diagnostic accuracy of myocardial perfusion imaging with single photon emission computed tomography and positron emission tomography: a comparison with coronary angiography. *Int J Cardiovasc Imaging* 2008; **24**: 511-518 [PMID: 18158612 DOI: 10.1007/s10554-007-9288-7]

11 **Bateman TM**, Heller GV, McGhie AI, Friedman JD, Case JA, Bryngelson JR, Hertenstein GK, Moutray KL, Reid K, Cullom SJ. Diagnostic accuracy of rest/stress ECG-gated Rb-82 myocardial perfusion PET: comparison with ECG-gated Tc-99m sestamibi SPECT. *J Nucl Cardiol* 2006; **13**: 24-33 [PMID: 16464714]

12 **Soulis JV**, Farmakis TM, Giannoglou GD, Louridas GE. Wall shear stress in normal left coronary artery tree. *J Biomech* 2006; **39**: 742-749 [PMID: 16439244 DOI: 10.1016/j.jbiomech.2004.12.026]

13 **Shanmugavelayudam SK**, Rubenstein DA, Yin W. Effect of geometrical assumptions on numerical modeling of coronary blood flow under normal and disease conditions. *J Biomech Eng* 2010; **132**: 061004 [PMID: 20887029 DOI: 10.1115/1.4001033]

14 **Katritsis DG**, Theodorakakos A, Pantos I, Andriotis A, Efstathopoulos EP, Siontis G, Karcanias N, Redwood S, Gavaises M. Vortex formation and recirculation zones in left anterior descending artery stenoses: computational fluid dynamics analysis. *Phys Med Biol* 2010; **55**: 1395-1411 [PMID: 20150685 DOI: 10.1088/0031-9155/55/5/009]

15 **Sun Z**, Choo GH, Ng KH. Coronary CT angiography: current status and continuing challenges. *Br J Radiol* 2012; **85**: 495-510 [PMID: 22253353 DOI: 10.1259/bjr/15296170]

16 **Mowatt G**, Cook JA, Hillis GS, Walker S, Fraser C, Jia X, Waugh N. 64-Slice computed tomography angiography in the diagnosis and assessment of coronary artery disease: systematic review and meta-analysis. *Heart* 2008; **94**: 1386-1393 [PMID: 18669550 DOI: 10.1136/hrt.2008.145292]

17 **Stein PD**, Yaekoub AY, Matta F, Sostman HD. 64-slice CT for diagnosis of coronary artery disease: a systematic review. *Am J Med* 2008; **121**: 715-725 [PMID: 18691486 DOI: 10.1016/j.amjmed.2008.02.039]

18 **Otero HJ**, Steigner ML, Rybicki FJ. The "post-64" era of coronary CT angiography: understanding new technology from physical principles. *Radiol Clin North Am* 2009; **47**: 79-90 [PMID: 19195535 DOI: 10.1016/j.rcl.2008.11.001]

19 **Hurlock GS**, Higashino H, Mochizuki T. History of cardiac computed tomography: single to 320-detector row multislice computed tomography. *Int J Cardiovasc Imaging* 2009; **25** Suppl 1: 31-42 [PMID: 19145476 DOI: 10.1007/s10554-008-9408-z]

20 **Abdulla J**, Asferg C, Kofoed KF. Prognostic value of absence or presence of coronary artery disease determined by 64-slice computed tomography coronary angiography a systematic review and meta-analysis. *Int J Cardiovasc Imaging* 2011; **27**: 413-420 [PMID: 20549366 DOI: 10.1007/s10554-010-9652-x]

21 **van Werkhoven JM**, Gaemperli O, Schuijf JD, Jukema JW, Kroft LJ, Leschka S, Alkadhi H, Valenta I, Pundziute G, de Roos A, van der Wall EE, Kaufmann PA, Bax JJ. Multislice computed tomography coronary angiography for risk stratification in patients with an intermediate pretest likelihood. *Heart* 2009; **95**: 1607-1611 [PMID: 19581272 DOI: 10.1136/hrt.2009.167353]

22 **Liu YC**, Sun Z, Tsay PK, Chan T, Hsieh IC, Chen CC, Wen MS, Wan YL. Significance of coronary calcification for prediction of coronary artery disease and cardiac events based on 64-slice coronary computed tomography angiography. *Biomed Res Int* 2013; **2013**: 472347 [PMID: 23586041 DOI: 10.1155/2013/472347]

23 **Silber S**, Albertsson P, Avilés FF, Camici PG, Colombo A, Hamm C, Jørgensen E, Marco J, Nordrehaug JE, Ruzyllo W, Urban P, Stone GW, Wijns W. Guidelines for percutaneous coronary interventions. The Task Force for Percutaneous Coronary Interventions of the European Society of Cardiology. *Eur Heart J* 2005; **26**: 804-847 [PMID: 15769784 DOI: 10.1093/eurheartj/ehi138]

24 **Smith SC**, Feldman TE, Hirshfeld JW, Jacobs AK, Kern MJ, King SB, Morrison DA, O'Neil WW, Schaff HV, Whitlow PL, Williams DO, Antman EM, Adams CD, Anderson JL, Faxon DP, Fuster V, Halperin JL, Hiratzka LF, Hunt SA, Nishimura R, Ornato JP, Page RL, Riegel B. ACC/AHA/SCAI 2005 guideline update for percutaneous coronary intervention: a report of the American College of Cardiology/American Heart Association Task Force on Practice Guidelines (ACC/AHA/SCAI Writing Committee to Update 2001 Guidelines for Percutaneous Coronary Intervention). *Circulation* 2006; **113**: e166-e286 [PMID: 16490830 DOI: 10.1161/CIRCULATIONAHA.106.173220]

25 **Jeetley P**, Burden L, Stoykova B, Senior R. Clinical and economic impact of stress echocardiography compared with exercise electrocardiography in patients with suspected acute coronary syndrome but negative troponin: a prospective randomized controlled study. *Eur Heart J* 2007; **28**: 204-211 [PMID: 17227784 DOI: 10.1093/eurheartj/ehl444]

26 **Shah BN**, Balaji G, Alhajiri A, Ramzy IS, Ahmadvazir S, Senior R. Incremental diagnostic and prognostic value of contemporary stress echocardiography in a chest pain unit: mortality and morbidity outcomes from a real-world setting. *Circ Cardiovasc Imaging* 2013; **6**: 202-209 [PMID: 23258477 DOI: 10.1161/CIRCIMAGING.112.980797]

27 **Cheng W**, Zeng M, Arellano C, Mafori W, Goldin J, Krishnam M, Ruehm SG. Detection of myocardial perfusion abnormalities: standard dual-source coronary computed tomography angiography versus rest/stress technetium-99m single-photo emission CT. *Br J Radiol* 2010; **83**: 652-660 [PMID: 20413446 DOI: 10.1259/bjr/82257160]

28 **Schwarz F**, Ruzsics B, Schoepf UJ, Bastarrika G, Chiaramida SA, Abro JA, Brothers RL, Vogt S, Schmidt B, Costello P, Zwerner PL. Dual-energy CT of the heart--principles and protocols. *Eur J Radiol* 2008; **68**: 423-433 [PMID: 19008064 DOI: 10.1016/j.ejrad.2008.09.010]

29 **Ruzsics B**, Schwarz F, Schoepf UJ, Lee YS, Bastarrika G, Chiaramida SA, Costello P, Zwerner PL. Comparison of dual-energy computed tomography of the heart with single photon emission computed tomography for assessment of coronary artery stenosis and of the myocardial blood supply. *Am J Cardiol* 2009; **104**: 318-326 [PMID: 19616661 DOI: 10.1016/j.amjcard.2009.03.051]

30 **Nagao M**, Kido T, Watanabe K, Saeki H, Okayama H, Kurata A, Hosokawa K, Higashino H, Mochizuki T. Functional assessment of coronary artery flow using adenosine stress dual-energy CT: a preliminary study. *Int J Cardiovasc Imaging* 2011; **27**: 471-481 [PMID: 20686853 DOI: 10.1007/s10554-010-9676-2]

31 **Kitagawa T**, Yamamoto H, Horiguchi J, Ohhashi N, Tadehara F, Shokawa T, Dohi Y, Kunita E, Utsunomiya H, Kohno N, Kihara Y. Characterization of noncalcified coronary plaques and identification of culprit lesions in patients with acute coronary syndrome by 64-slice computed tomography. *JACC Cardiovasc Imaging* 2009; **2**: 153-160 [PMID: 19356549 DOI: 10.1016/j.jcmg.2008.09.015]

32 **Takumi T**, Lee S, Hamasaki S, Toyonaga K, Kanda D, Kusumoto K, Toda H, Takenaka T, Miyata M, Anan R, Otsuji Y, Tei C. Limitation of angiography to identify the culprit plaque in acute myocardial infarction with coronary total occlusion utility of coronary plaque temperature measurement to identify the culprit plaque. *J Am Coll Cardiol* 2007; **50**: 2197-2203 [PMID: 18061065]

33 **Lee BK**. Computational fluid dynamics in cardiovascular disease. *Korean Circ J* 2011; **41**: 423-430 [PMID: 21949524 DOI: 10.4070/kcj.2011.41.8.423]

34 **Tu J**, Yeoh GH, Liu C. Computational Fluid dynamics. A Practical Approach. 1st ed. Oxford: Elesevier, 2008: 1-27

35 **Caro CG**, Fitz-Gerald JM, Schroter RC. **Arterial wall shear** and distribution of early atheroma in man. *Nature* 1969; **223**: 1159-1160 [PMID: 5810692]

36 **Malek AM**, Alper SL, Izumo S. Hemodynamic shear stress and its role in atherosclerosis. *JAMA* 1999; **282**: 2035-2042 [PMID: 10591386 DOI: 10.1001/jama.282.21.2035]

37 **Perktold K**, Resch M, Peter RO. **Three-dimensional numerical** analysis of pulsatile flow and wall shear stress in the carotid artery bifurcation. *J Biomech* 1991; **24**: 409-420 [PMID: 1856241]

38 **Lei M**, Archie JP, Kleinstreuer C. Computational design of a bypass graft that minimizes wall shear stress gradients in the region of the distal anastomosis. *J Vasc Surg* 1997; **25**: 637-646 [PMID: 9129618]

39 **Perktold K**, Rappitsch G. Computer simulation of local blood flow and vessel mechanics in a compliant carotid artery bifurcation model. *J Biomech* 1995; **28**: 845-856 [PMID: 7657682]

40 **Steinman DA**, Ethier CR. The effect of wall distensibility on flow in a two-dimensional end-to-side anastomosis. *J Biomech Eng* 1994; **116**: 294-301 [PMID: 7799630]

41 **Knight J**, Olgac U, Saur SC, Poulikakos D, Marshall W, Cattin PC, Alkadhi H, Kurtcuoglu V. Choosing the optimal wall shear parameter for the prediction of plaque location-A patient-specific computational study in human right coronary arteries. *Atherosclerosis* 2010; **211**: 445-450 [PMID: 20466375 DOI: 10.1016/j.atherosclerosis.2010.03.001]

42 **Wellnhofer E**, Osman J, Kertzscher U, Affeld K, Fleck E, Goubergrits L. Flow simulation studies in coronary arteries--impact of side-branches. *Atherosclerosis* 2010; **213**: 475-481 [PMID: 20934704 DOI: 10.1016/j.atherosclerosis.2010.09.007]

43 **Chaichana T**, Sun Z, Jewkes J. Impact of plaques in the left coronary artery on wall shear stress and pressure gradient in coronary side branches. *Comput Methods Biomech Biomed Engin* 2014; **17**: 108-118 [PMID: 22443493 DOI: 10.1080/10255842.2012.671308]

44 **Rikhtegar F**, Knight JA, Olgac U, Saur SC, Poulikakos D, Marshall W, Cattin PC, Alkadhi H, Kurtcuoglu V. Choosing the optimal wall shear parameter for the prediction of plaque location-A patient-specific computational study in human left coronary arteries. *Atherosclerosis* 2012; **221**: 432-437 [PMID: 22317967 DOI: 10.1016/j.atherosclerosis.2012.01.018]

45 **Wong K**, Mazumdar J, Pincombe B, Worthley SG, Sanders P, Abbott D. Theoretical modeling of micro-scale biological phenomena in human coronary arteries. *Med Biol Eng Comput* 2006; **44**: 971-982 [PMID: 17048027 DOI: 10.1007/s11517-006-0113-6]

46 **Katritsis D**, Kaiktsis L, Chaniotis A, Pantos J, Efstathopoulos EP, Marmarelis V. Wall shear stress: theoretical considerations and methods of measurement. *Prog Cardiovasc Dis* 2007; **49**: 307-329 [PMID: 17329179 DOI: 10.1016/j.pcad.2006.11.001]

47 **Rodriguez-Granillo GA**, García-García HM, Wentzel J, Valgimigli M, Tsuchida K, van der Giessen W, de Jaegere P, Regar E, de Feyter PJ, Serruys PW. Plaque composition and its relationship with acknowledged shear stress patterns in coronary arteries. *J Am Coll Cardiol* 2006; **47**: 884-885 [PMID: 16487861 DOI: 10.1016/j.jacc.2005.11.027]

48 **Chaichana T**, Sun Z, Jewkes J. Computation of hemodynamics in the left coronary artery with variable angulations. *J Biomech* 2011; **44**: 1869-1878 [PMID: 21550611 DOI: 10.1016/j.jbiomech.2011.04.033]

49 **Sun Z**, Cao Y. Multislice CT angiography assessment of left coronary artery: correlation between bifurcation angle and dimensions and development of coronary artery disease. *Eur J Radiol* 2011; **79**: e90-e95 [PMID: 21543178 DOI: 10.1016/j.ejrad.2011.04.015]

50 **Fuster V**. Lewis A. Conner Memorial Lecture. Mechanisms leading to myocardial infarction: insights from studies of vascular biology. *Circulation* 1994; **90**: 2126-2146 [PMID: 7718033]

51 **Gziut AI**. [Comparative analysis of atherosclerotic plaque distribution in the left main coronary artery and proximal segments of left anterior descending and left circumflex arteries in patients qualified for percutaneous coronary angioplasty]. *Ann Acad Med Stetin* 2006; **52**: 51-62; discussion 62-63 [PMID: 17633397]

52 **Han SH**, Puma J, García-García HM, Nasu K, Margolis P, Leon MB, Lerman A. Tissue characterisation of atherosclerotic plaque in coronary artery bifurcations: an intravascular ultrasound radiofrequency data analysis in humans. *EuroIntervention* 2010; **6**: 313-320 [PMID: 20884408 DOI: 10.4244/EIJV6I3A53]

53 **Gijsen FJ**, Wentzel JJ, Thury A, Lamers B, Schuurbiers JC, Serruys PW, van der Steen AF. A new imaging technique to study 3-D plaque and shear stress distribution in human coronary artery bifurcations in vivo. *J Biomech* 2007; **40**: 2349-2357 [PMID: 17335832 DOI: 10.1016/j.jbiomech.2006.12.007]

54 **Grayburn PA**, Willard JE, Haagen DR, Brickner ME, Alvarez LG, Eichhorn EJ. Measurement of coronary flow using high-frequency intravascular ultrasound imaging and pulsed Doppler velocimetry: in vitro feasibility studies. *J Am Soc Echocardiogr* 1992; **5**: 5-12 [PMID: 1531416]

55 **Rodriguez-Granillo GA**, Rosales MA, Degrossi E, Durbano I, Rodriguez AE. Multislice CT coronary angiography for the detection of burden, morphology and distribution of atherosclerotic plaques in the left main bifurcation. *Int J Cardiovasc Imaging* 2007; **23**: 389-392 [PMID: 17028928 DOI: 10.1007/s10554-006-9144-1]

56 **Chaichana T**, Sun Z, Jewkes J. Hemodynamic impacts of various types of stenosis in the left coronary artery bifurcation: a patient-specific analysis. *Phys Med* 2013; **29**: 447-452 [PMID: 23453845 DOI: 10.1016/j.ejmp.2013.02.001]

57 **Pijls NH**, De Bruyne B, Peels K, Van Der Voort PH, Bonnier HJ, Bartunek J Koolen JJ, Koolen JJ. Measurement of fractional flow reserve to assess the functional severity of coronary-artery stenoses. *N Engl J Med* 1996; **334**: 1703-1708 [PMID: 8637515]

58 **Watkins S**, McGeoch R, Lyne J, Steedman T, Good R, McLaughlin MJ, Cunningham T, Bezlyak V, Ford I, Dargie HJ, Oldroyd KG. Validation of magnetic resonance myocardial perfusion imaging with fractional flow reserve for the detection of significant coronary heart disease. *Circulation* 2009; **120**: 2207-2213 [PMID: 19917885 DOI: 10.1161/CIRCULATIONAHA.109.872358]

59 **Berger A**, Botman KJ, MacCarthy PA, Wijns W, Bartunek J, Heyndrickx GR, Pijls NH, De Bruyne B. Long-term clinical outcome after fractional flow reserve-guided percutaneous coronary intervention in patients with multivessel disease. *J Am Coll Cardiol* 2005; **46**: 438-442 [PMID: 16053955 DOI: 10.1016/j.jacc.2005.04.041]

60 **Kristensen TS**, Engstrøm T, Kelbæk H, von der Recke P, Nielsen MB, Kofoed KF. Correlation between coronary computed tomographic angiography and fractional flow reserve. *Int J Cardiol* 2010; **144**: 200-205 [PMID: 19427706 DOI: 10.1016/j.ijcard.2009.04.024]

61 **Min JK**, Leipsic J, Pencina MJ, Berman DS, Koo BK, van Mieghem C, Erglis A, Lin FY, Dunning AM, Apruzzese P, Budoff MJ, Cole JH, Jaffer FA, Leon MB, Malpeso J, Mancini GB, Park SJ, Schwartz RS, Shaw LJ, Mauri L. Diagnostic accuracy of fractional flow reserve from anatomic CT angiography. *JAMA* 2012; **308**: 1237-1245 [PMID: 22922562 DOI: 10.1001/2012.jama.11274]

62 **Koo BK**, Erglis A, Doh JH, Daniels DV, Jegere S, Kim HS, Dunning A, DeFrance T, Lansky A, Leipsic J, Min JK. Diagnosis of ischemia-causing coronary stenoses by noninvasive fractional flow reserve computed from coronary computed tomographic angiograms. Results from the prospective multicenter DISCOVER-FLOW (Diagnosis of Ischemia-Causing Stenoses Obtained Via Noninvasive Fractional Flow Reserve) study. *J Am Coll Cardiol* 2011; **58**: 1989-1997 [PMID: 22032711 DOI: 10.1016/j.jacc.2011.06.066]

63 **Yoon YE**, Choi JH, Kim JH, Park KW, Doh JH, Kim YJ, Koo BK, Min JK, Erglis A, Gwon HC, Choe YH, Choi DJ, Kim HS, Oh BH, Park YB. Noninvasive diagnosis of ischemia-causing coronary stenosis using CT angiography: diagnostic value of transluminal attenuation gradient and fractional flow reserve computed from coronary CT angiography compared to invasively measured fractional flow reserve. *JACC Cardiovasc Imaging* 2012; **5**: 1088-1096 [PMID: 23153908 DOI: 10.1016/j.jcmg.2012.09.002]

64 **Grunau GL**, Min JK, Leipsic J. Modeling of fractional flow reserve based on coronary CT angiography. *Curr Cardiol Rep* 2013; **15**: 336 [PMID: 23264169 DOI: 10.1007/s11886-012-0336-0]

65 **Min JK**, Berman DS, Budoff MJ, Jaffer FA, Leipsic J, Leon MB, Mancini GB, Mauri L, Schwartz RS, Shaw LJ. Rationale and design of the DeFACTO (Determination of Fractional Flow Reserve by Anatomic Computed Tomographic AngiOgraphy) study. *J Cardiovasc Comput Tomogr* 2011; **5**: 301-309 [PMID: 21930103 DOI: 10.1016/j.jcct.2011.08.003]

66 **Lee BK**, Kwon HM, Hong BK, Park BE, Suh SH, Cho MT, Lee CS, Kim MC, Kim CJ, Yoo SS, Kim HS. Hemodynamic effects on atherosclerosis-prone coronary artery: wall shear stress/rate distribution and impedance phase angle in coronary and aortic circulation. *Yonsei Med J* 2001; **42**: 375-383 [PMID: 11519078]

67 **Friedman MH**, Deters OJ, Mark FF, Bargeron CB, Hutchins GM. Arterial geometry affects hemodynamics. A potential risk factor for athersoclerosis. *Atherosclerosis* 1983; **46**: 225-231 [PMID: 6838702]

68 **Felsenthal G**, Butler DH, Shear MS. Across-tarsal-tunnel motor-nerve conduction technique. *Arch Phys Med Rehabil* 1992; **73**: 64-69 [PMID: 1729977]

69 **Lee BK**, Kwon HM, Kim D, Yoon YW, Seo JK, Kim IJ, Roh HW, Suh SH, Yoo SS, Kim HS. Computed numerical analysis of the biomechanical effects on coronary atherogenesis using human hemodynamic and dimensional variables. *Yonsei Med J* 1998; **39**: 166-174 [PMID: 9587258]

70 **Pijls NH**, van Schaardenburgh P, Manoharan G, Boersma E, Bech JW, van't Veer M, Bär F, Hoorntje J, Koolen J, Wijns W, de Bruyne B. Percutaneous coronary intervention of functionally nonsignificant stenosis: 5-year follow-up of the DEFER Study. *J Am Coll Cardiol* 2007; **49**: 2105-2111 [PMID: 17531660 DOI: 10.1016/j.jacc.2007.01.087]

P- Reviewers: Peteiro J, Rodriguez-Granillo GA, Ueda H
S- Editor: Zhai HH **L- Editor**: A **E- Editor**: Liu XM